pH, Geoelectrical and Membrane Flux Parameters for the Monitoring of Water-Saturated Silicate and Carbonate Porous Media contaminated by CO_2

Luqman K. Abidoye, Diganta Bhusan Das*

Chemical Engineering Department, Loughborough University, Loughborough, Leicestershire, LE11 3TU, United Kingdom

(*Corresponding author; Email: D.B.Das@lboro.ac.uk; Phone: 0044 1509 222509)

Abstract

Characteristics of potable water aquifer contaminated by CO_2 are investigated using well-defined laboratory experiments. The porous media domain was prepared with silica sand and limestone in separate experiments. The investigations used combinations of techniques to measure various parameters in the water-saturated porous media domain on which pressure of CO_2 was imposed, under various conditions, which correspond to different geological depths. Measured parameters included the pH, geoelectrical parameters, and the diffusion of the CO_2 gas through the water-saturated porous media domain using non-porous silicone rubber sheet. Experimental results revealed the existence of three stages in the profile of pH change with time as CO_2 dissolved and diffused in the water-saturated porous media domain, which was composed of silica sand. The first stage was characterised by rapid decline in the pH. This is associated with quick dissolution of CO_2 and the formation of carbonic acid together with bicarbonate. The second stage showed short rise in pH value, which was attributed to the reverse reaction, i.e., the formation of aqueous and gaseous CO_2 and water from the carbonic acid. The third stage was that of the equilibrium in the forward and the reverse reactions, marked by steady state in pH value, which remained unchanged till the end of the experiment. The bulk electrical conductivity (σ_b) of the water-saturated porous domain increased in the presence of CO_2. This is attributed to the formation of ionic species, especially bicarbonate, as CO_2 dissolved in the domain. The rise in σ_b coincided with the first stage of the change in the pH of the system. In addition, the σ_b was higher in limestone than silica sand, and it increased with pressure of the domain. But, the bulk dielectric constant (ε_b) showed no change with the dissolution of the CO_2 under different conditions. Furthermore, permeation of CO_2 through the silicone rubber indicated the diffusion of the CO_2 gas through the water-saturated domain. CO_2 flux through the membrane was shown to increase with depth or pressure of the domain. A mathematical

expression derived in this work shows the dependence of σ_b on the pH and the initial value of $\sigma_{b.}$ Predictions of the changes in the σ_b for different porous domains show the reliability of the mathematical expression developed in this work.

Keywords: $CO_{2,}$ silicate, carbonate, pH, electrical conductivity, dielectric constant

Nomenclature

J	Mass transfer rate per unit area	$kgm^{-2}hr^{-1}$
K	Intrinsic permeability of porous medium	m^2
m	Mass of gas	kg
t	Time	hr
D_p	Average particle diameter	m
TDR	Time domain reflectometry	-
PT	Pressure transducer	-
σ_b	Bulk electrical conductivity	$(\Omega m)^{-1}$
σ_{bi}	Initial value of σ_b before the injection of CO_2	-
σ_{br}	Ratio of the steady state value of σ_b to the initial value of σ_b (σ_{bi})	-
ϵ_b	Bulk dielectric constant	-
ϕ	Porosity of porous medium	-

1.0 Introduction

Geological carbon sequestration has been proposed as a possible approach, which can significantly limit the amount of CO_2 in the atmosphere [1]–[3]. However, the goal of the sequestration may be compromised by leakage of stored CO_2 which can take place due to high permeability pathways around the existing well bore [4], nearby leaky wells [5], [6], fractures around caprocks [7], wettability alteration of the caprocks [8], and so on. In certain circumstances, it is feared that the vertical or upward migration of the leaked CO_2 from the sequestrated aquifer may encounter overlying aquifers with potable water resulting in contamination of the water [5], [9], [10].

The assurance of a secure geological carbon sequestration practice should be accompanied with deployment of monitoring technologies and approaches that detect the movement of the CO_2 plume around the CO_2 storage formation before possible contamination of the potable water resources [10], [11]. Characteristics of the potable water contaminated by CO_2 can be determined using various combinations of techniques and tools. Methods based on geoelectrical measurement techniques [12]–[15], pH measurements [10], [12], [13], and membrane sensor [11] have been used to study the scenarios of CO_2 migration or water contamination by CO_2 in the subsurface.

Dethlefsen et al. [10] state that the most significant geochemical processes, which occur during the CO_2 contamination of potable water are the changes in the pH and the resultant changes in the electrical conductivity (σ) of the fluid-fluid-porous media system (i.e., CO_2-water-porous media system). A lowering of pH during CO_2 dissolution in water is attributed to the formation of carbonic acid, which increases with the partial pressure of the CO_2 [13]. The change in σ during the process is attributed to mineral dissolution from the rock/porous material, which is more pronounced in carbonate formation. The dynamics of the change in electrical characteristics of CO_2-contaminated water in the aquifer is discussed by Dafflon et al. [13]. They show the impact of the transition between bicarbonate and carbonic acid in the CO_2-contaminated water on the electrical resistivity of the system. An increase in the amount of dissolved CO_2 was shown to lead to an initial decrease in the resistivity as a result of an increase in the amounts of bicarbonate and dissolved species in the system. Following the initial decrease in its value, the resistivity value rises at higher partial pressure of CO_2 in a process attributed to the continued lowering of pH and the related transition of bicarbonate into non-dissociated carbonic acid, which reduces the total concentration of dissociated species [13]. Dethlefsen et al. [10] show that the change in σ is detectable with geoelectric measurement. The detectability is enhanced by the dissolution of the carbonate, and is reduced in the non-calcareous aquifers. Yang et al. [12] developed multicomponent geochemical model that simulated CO_2 dissolution in groundwater, aqueous complexation, mineral reactions (dissolution/precipitation), and surface complexation on clay mineral surfaces. Their study has shown that there is greater threat of groundwater acidification in non-carbonate aquifer in the presence of CO_2. A number of authors (see, e.g., [10]) acknowledge the need for the evaluation of the sensitivity of geoelectric measurement technique, with respect to the variations in the geological parameters and boundary conditions of the CO_2. Earlier, Drnevich et al. [16] investigated the effect of temperature on dielectric constant (ε) of water in porous media. Their findings show that ε decreases with increase in temperature. But, the study was conducted under atmospheric condition with only one liquid phase (water) present in the porous medium.

The work of Zimmer et al. [11] shows the application of silicone rubber as a selective membrane in conjunction with other analytical instruments for the detection of gases present in the underground and borehole. Their work was related to the carbon sequestration project (CO_2SINK) at Ketzin, Germany. They successfully demonstrate the detection of CO_2 front at observation wells, located at different distances to the injection well, using the gas membrane sensor system.

Considering the above points, the applications of the geoelectric techniques, pH measurements and gas permeation through membrane in the monitoring of the potable water aquifer contaminated by CO_2 can be appreciated. However, some of the above studies were conducted under or near ambient conditions (see e.g.,[13], [16]). Also, the studies were mainly conducted in sediments consisting of mixture of materials and metals making it difficult to distinguish the influence of pure minerals and metal content on the measurements made.

From a flow system point of view, the CO_2 contamination of the potable water aquifers can be visualised as two-phase static system with the water in porous media remaining static while the contaminating plume of CO_2 imposed a pressure head at the boundary [5], [17]. However, some of the experiments in the above-cited publications consider the detection of the CO_2 as a contaminant alone (see e.g., [11] rather than the effects of the contamination on the potable water in the aquifer.

In the light of the foregoing discussions, one can easily acknowledge the threat posed by leakage of CO_2 from storage aquifer on the potable water aquifer that might lie on its path. The migration of leaked CO_2 from the sequestrated site will pass through layers of geological sediments, where potable water aquifers might be found. This scenario calls for the investigations of the behaviour of the CO_2-contaminated water in the porous media at different temperatures and pressures corresponding to different geological depths in which potable water aquifers might be found in the geological domain. Furthermore, common geological aquifers are rich in silicate and/or carbonate minerals [10], [18]–[21]. These minerals might influence the characteristics of the potable water in the aquifers contaminated by CO_2. Therefore, it is necessary to conduct investigations with well-characterised porous media (e.g., using silicate or carbonate rich materials).

To bridge the above-identified gaps in the current knowledge, this work aims to utilize well-characterised unconsolidated porous media, rich in silicate and carbonate minerals, respectively, to investigate the characteristics of the water-saturated porous media contaminated by CO_2. Investigation methods to be used include pH measurements, application of silicone rubber as a membrane in the monitoring of CO_2 diffusion in the contaminated water-saturated porous media, and the geoelectrical measurement techniques for the determination of the bulk dielectric constant (ε_b) and the bulk electrical conductivity (σ_b) of the CO_2-water-porous media system. The investigations are designed to mimic contamination of the potable water aquifer by CO_2 at different geological depths. Thus,

different pressure and temperature of CO_2 are imposed on the experimental domain. This design satisfies the call by Dethlefsen et al. [10] for the evaluation of the sensitivity of the boundary conditions of CO_2 on geoelectrical measurement methods. Unlike the works discussed above, this paper discusses simultaneous measurements of pH, geoelectrical parameters and gas permeation through membrane, as a comprehensive procedure for the monitoring of the water-saturated silicate and carbonate porous media contaminated by CO_2.

In this work, porous media domain was prepared using well-characterised particles of silica sand and limestone. The domain was used in the experimental investigations of the effects of CO_2 contamination on the water-saturated porous media. This work involves the measurements of the pH and geoelectrical parameters (ε_b and σ_b) to monitor changes in the characteristics of the water-saturated porous media contaminated by CO_2. The permeation of CO_2 through the nonporous silicone rubber was also recorded using a membrane-sensor system. The results of the investigations are discussed in relation to different geological depths where potable water aquifers might be encountered by plume of CO_2 migrating from storage aquifer, where leakage occurs. Time domain reflectometry (TDR) method was used to measure the bulk dielectric constant (ε_b), and the bulk electrical conductivity (σ_b) of the CO_2-water-porous media system. Further details about the TDR measurement techniques and principles are expatiated in the methodology section.

2. Methodology

2.1 Porous domain and materials

The experiments in this work were conducted using two materials, namely, silica sand and limestone particles. They have been chosen so as to provide two porous domains (silicate and carbonate domains) with different chemical but similar physical properties for separate experiments. The silica sand was purchased from Minerals Marketing (Buxton, UK), while the limestone was purchased from the Tarmac Buxton Lime and Cement (Buxton, UK). The physical and chemical properties of the samples are listed in Table 1. From the table, it can be seen that the physical properties of the two materials are very similar. Constant-head permeameter technique [22] was used to determine the permeability of the packed particle bed. Before use, the porous domains were pre-treated by washing in tap water and dried for at least 24 hours to remove any clay content. To ensure uniform particle deposition in every experiment, the sand was poured through a large sieve into the cell, which initially contains water to minimise air trap. The characterizations of the water-saturated porous media in the presence of CO_2 relied on the measurements of the system electrical parameters, pH and

CO_2 permeation through non-porous silicone rubber membrane. The silicone rubber sheet (part number: RS 340-2689) used in our gas permeation experiments was obtained from RS Components Ltd (Northants, UK) with the thickness of 3mm.

2.2 Instrumentations and sample holder

In situ bulk dielectric constant and electrical conductivity measurements were made with the three-pin time domain reflectometry probes (TDR probes). The TDR probes were locally constructed in our laboratory and held together with high temperature PTFE base holder for use under high pressure and high temperature conditions. The probe rods were insulated in the regions of contact with the steel body of the sample holder to avoid interference of the signal. The TDR probes cables were connected to a multiplexer, which was attached to electrical impulse generator - TDR100 reflectometer (Campbell Scientific Ltd, Shepshed, UK). This was then connected to CR10X datalogger (Campbell Scientific Ltd, Shepshed, UK) for automatic collection and storage of data collected from the TDR probes inserted into the porous medium. 12V and 50 Hz dual rail power supply (Rapid Electronics Ltd, Essex, UK) was used to supply power to a datalogger. At the start of the experiment, the TDR probes were calibrated to get the offset and multiplier following the Campbell Scientific instruction manual. The calibration results were used in developing the program used in communicating the TDR100 to the datalogger. The TDR100 has a timing resolution of 12.2 picoseconds for 2-way travel and the pulse length of 14 microseconds.

Figure 1A is a schematic diagram of the experimental set up. The figure indicates the port for the TDR probes at the centre of the sample holder. Two pressure transducers (PTs) HySense PR 140 (Hydrotechnik, GmbH, Limburg an der Lahn, Germany) were included at the directly opposite ports at the centre of the domain. The PTs were held in steel holders together with the silicone rubber membranes. The arrangement permits the *in situ* measurement of the pressure of CO_2 that diffuses through the water-saturated porous domain and permeates through the membrane. Fresh samples of silicone rubber were used at the start of each experiment. The sample holder was situated in a heating cabinet to maintain predetermined temperature in the system. Electric heaters were placed at the corners of the heating cabinet while the system temperature was regulated using PID temperature controller (West Control Solutions, Brighton, UK). The sample holder is a 4cm high stainless steel cell with 10cm diameter having stainless steel end-pieces at the top and the bottom.

Table 1: Properties of the sand bed and particles

Porous Sample / Properties	Limestone Particles (Trucal 6)	Silica Particles (DA14/25)
Permeability, K (m^2)	4.53×10^{-10}	3.65×10^{-10}
Particle Bed Porosity, ϕ (-)	0.39	0.37
Particle Density, (kgm^{-3})	2690	2740
Average Particle Diameter, D_p (µm)	1200	946.1
SiO_2 Content (%)	-	99[a]
$CaCO_3$ Content (%)	>98[b]	-

[a] www.sibelco.co.uk (accessed May 2014)

[b] www.lafargetarmac.com (accessed May 2014)

Figure 1B shows the photograph of the sample holder filled with silica sand, PTs plugged at ports as well as the TDR probes at the designated port at the centre of the sample holder. Figure 1C shows the photograph of the steel holder, holding the PT and the silicone rubber membrane together. Narrow steel tubes run upstream and downstream of the sample holder. The inner parts of the top and bottom end pieces are overlaid with hydrophobic polytetrafluoroethylene, PTFE (0.1µm) and hydrophilic nylon (1µm), respectively. The membranes were purchased from Porvair Filtration Group Ltd (Hampshire, UK). The PTFE was used to prevent excursion of water from the water-saturated domain in the sample holder into the supercritical fluid pump while the nylon was used to minimise CO_2 exit from the bottom of the sample holder. It was reported that hydrophilic nylon membrane minimises CO_2 escape from the bottom of the sample holder [23]. Distributor was used at the top of sand sample in the domain to ensure even distribution of the CO_2 at the top of the domain. Precision back pressure regulator (BPR) (Equilibar, Fletcher, USA) was situated at the downstream tube. It was used to minimize destabilization of the domain pressure whenever a sample was taken for pH analysis through the valve V-6 (see, Figure 1). The back pressure regulator was a dome loaded type using PTFE-glass diaphragm and was loaded with nitrogen gas from a nitrogen cylinder (BOC gases, Leicester, UK) controlled with a single stage regulator. The pH measurement was performed with the aid of the digital pH meter (Hydrus 500) (Fisher Scientific, Loughborough, UK).

2.3 Experimental Procedure

2.3.1 Equipment set up

All experiments were conducted in a 4cm sample holder cell. The sample holder was set up by placing the body of the sample holder on the bottom end piece (sample holder base). Ports on the sample holder were plugged with steel holders, which hold the PTs and the membrane. These were then connected to the peripheral devices as discussed above. A small amount of tap water was poured into the cell to a certain position followed by pouring of sand through a metal sieve of appropriate size to ensure uniform sand deposition and prevent air trap. Equal amount of sand (500g) was used in all experiments. A distributor was placed on the top of the sand bed. Then, the top end piece with the hydrophobic membrane was placed over the sand bed. After tightening all the tubing connection points, more tap water was passed into the sample from the water tank and pressurised up to the experimental set pressure using the hand pump (see Figure 1). At high pressure, all air present in the tubing and the sand was considered dissolved [23]. Water tank valve (V-4) was then closed. Level of the water in the tubing was then adjusted by letting off some water through the outlet valve, V-5. This was done to ensure that the water level stays at the surface of the sand bed in the sample holder, so that the incoming CO_2 will make contact with the water at the sand surface. CO_2 used in this work was obtained from BOC Industrial gases (Loughborough, UK) at 99.9% purity. The supercritical fluid pump (Teledyne Isco, Lincoln NE, USA) was filled with liquid CO_2 from the CO_2 cylinder by opening of the valve, V-1, and setting the pump on refill mode. When the pump tank was full, the CO_2 cylinder valve, V-1, was closed and the pressure on the supercritical fluid pump was raised to the experimental pressure while valve, V-2 remained closed. When the supercritical fluid pump was set at the experimental pressure, the heater was switched on and set at the experimental temperature. When the temperature and pressure are at equilibrium, valve, V-2 was opened and the CO_2 was supplied into the upstream tubing up to the top of the sand bed in the sample holder, forming interface with water-saturated domain.

2.3.2 Design of the experimental conditions

As explained under the introduction of this work, the experiments were designed to fulfil the conditions of temperature and pressure that are likely to be encountered by CO_2 migrating or escaping from geological sequestration site into the shallow subsurface. Figure 2 illustrates this scenario. In the figure, potable water aquifers are located at different depths in the sediment. The leaked CO_2 follows a pathway (e.g., fracture in caprock, high permeability pathway, etc.) to reach the water aquifer. The water aquifers in the figure can be viewed separately (i.e., one aquifer in one sediment) or collectively (i.e., all aquifers at different

depths of a single sediment). The hypothetical geological conditions were determined using the reports of the Best [24] for geobaric pressure gradients and that of the Nordbotten et al. [6] for warm basin geothermal gradient. The conditions were listed in Table 2. For safety concerns, the experiments were limited to conditions corresponding to 200m depth. In Table 2, temperature and pressure at which injections of CO_2 were done differ for each depth considered. This is because temperature and pressure vary together with depth in geological sediment [6], [24]. The table further shows the varying density and dynamic viscosity of CO_2 under different conditions. Under these conditions, the *in situ* measurements of the electrical parameters (bulk dielectric constant (ε_b) and the bulk electrical conductivity (σ_b)) and the responses of membrane-sensor system were conducted. But the pH measurements were conducted under atmospheric condition by immediate measurements of small sample taken from the domain.

Table 2: List of conditions which were experimentally simulated in our study

Depth (m)	**Temperature (^oC)**	**Pressure (bar)**	**CO_2 Density (kgm^{-3})**[a]	**CO_2 Dynamic viscosity (10^{-6} Pa s)**[a]
50	22.25	13.5	26.34	14.98
100	24.5	27	56.87	15.37
200	29	54	144.0	17.20

a. http://www.peacesoftware.de/einigewerte/co2_e.html

From a practical point of view, one may wonder whether membrane-sensor system can be successfully applied at deep geological sediment. Earlier, Lamert et al. [25] demonstrated the field measurements of electrical parameters to monitor the subsurface CO_2 movement. They installed several copper electrodes at various depths up to 18.5m below the ground level around the CO_2 injection site in order to monitor the movement of injected CO_2 in the space surrounding the injection site. Therefore, if copper electrodes can be buried at such geological depths, it is believed that miniaturised pressure sensor can be coupled with highly selective non-porous membrane at various depths for similar practical applications.

2.3.3 pH measurement

The pH of the solution was measured at intervals using the pH meter (Hydrus 500, Fisher Scientific, Loughborough, UK). At any particular time of interest, solution sample was taken by opening of the valve, V-6 (see, Figure 1). The BPR ensured that the system pressure

remained stable after short disturbance of the opening of the valve. The sample pH was immediately measured using the pH meter. The pH meter was regularly calibrated to ensure consistent and reliable measurements.

2.3.4 Time domain reflectometry

For the measurements of the geoelectrical parameters in the water-saturated domain contaminated by CO_2, time domain reflectometry (TDR) method was used [16], [25], [27]. The TDR probes serve as the waveguide extension on the coaxial cable connected to the TDR100 (electrical impulse generator). It will be recalled that the TDR probes used in this work are made in our workshop in order for them to be suitable for high temperature and pressure conditions of our work. But the impulse generator (TDR100) to which the cable of the TDR probes was connected, the multiplexer, and the datalogger are branded products (Campbell Scientific Ltd, Shepshed, UK). The TDR system was calibrated to determine the necessary parameters (e.g., offset and multiplier) following the instruction manual of Campbell Scientific Ltd (Shepshed, UK). The TDR100 generates the electrical pulses, which travel through the coaxial cable connected to the TDR probes. Owing to the contrast in impedance resulting from materials surrounding the TDR probes, reflections occur which are sent back to the source (TDR100). TDR100 samples and digitizes the reflection waveforms to infer the impedance value. The impedance value is related to the geometrical configuration of the probe and inversely related to the dielectric constant of the surrounding medium. Owing to sharp contrast between the dielectric constant of the porous medium and the surrounding fluids, a change in fluid content causes a change in the bulk dielectric constant, which is seen as a change in probe impedance affecting the shape of the reflected waveform. Information from the differences in shape of the reflection is used by the TDR measurement system to determine the bulk dielectric constant (ε_b) and the bulk electrical conductivity (σ_b) of the system.

2.3.5 Calculation of CO_2 flux through the non-porous membrane

To assess the performance of a membrane in term of the mass of gas that permeate through its matrix, Shahrabi et al. [28] describe the gas permeate flux (J) through the membrane as:

$$J = m/A.t \quad (1)$$

m (kg) is the total mass of the permeate at the experimental time interval, t (h), and A is the effective membrane area for permeation (m^2). The mass of the gas that permeates through the membrane was calculated by assuming the ideal gas relation for the CO_2. Since the gas volume of the membrane-sensor system is known while the pressure change (in the membrane-sensor system), as a result of the increase in the amount of permeated gas is

automatically recorded, the mass of the CO_2 present in the open volume of the membrane-sensor system can be readily determined, using the ideal gas equation.

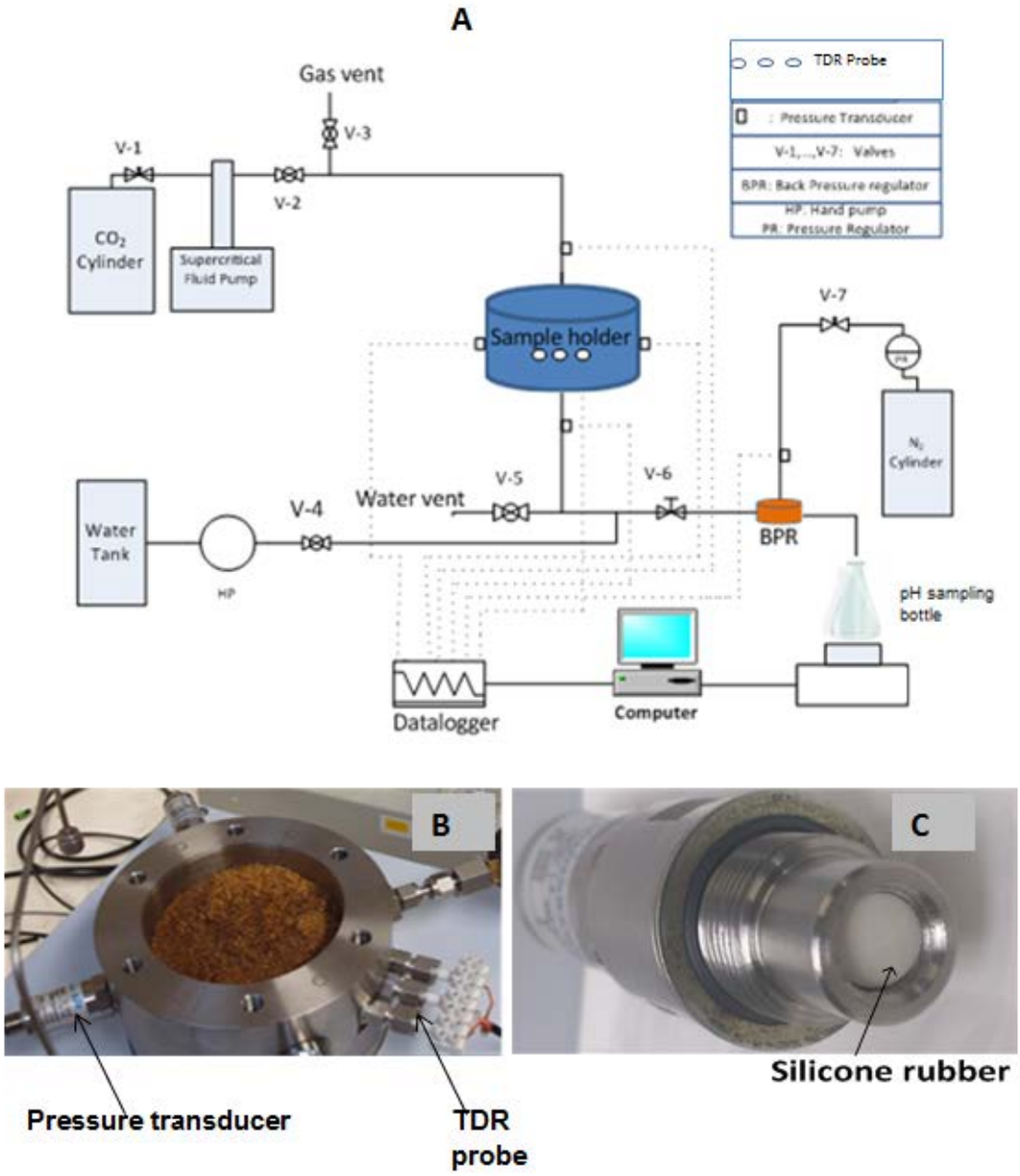

Figure 1: (A) Schematic diagram of experimental rig for the investigation of CO_2-contamination of water in porous media. (B) Photograph of the sample holder showing silica sand, pressure transducer and TDR (C) Steel holder showing the pressure transducer and the silicone rubber sheet (metal cap not shown). Sample holder size: internal diameter=10cm, sample height=4cm.

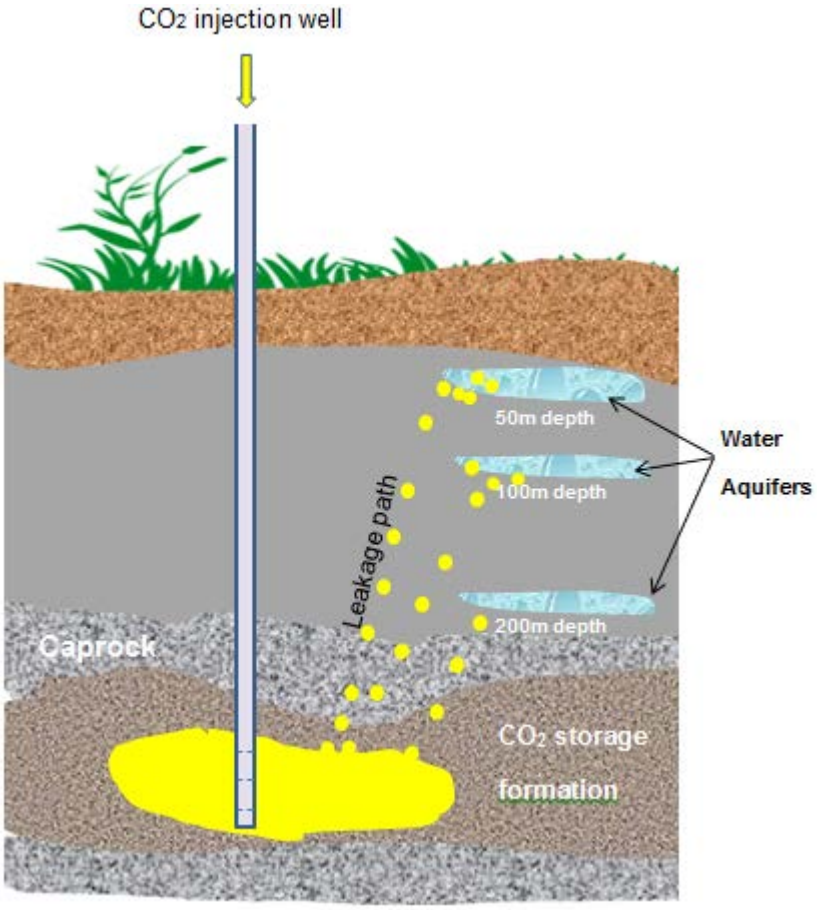

Figure 2: Hypothetical representation of geological sediment with potable water aquifers located at different depths. This work considers effect of aquifer depth on CO_2 contamination of water-saturated aquifer.

3.0 Results and discussions

As we have explained earlier, the leakage of CO_2 from geological carbon sequestration aquifer may result in the contamination of potable water aquifers that lie above the aquifer [4], [10], [21]. This will affect the pH and the electrical properties of the water-filled porous media, as a result of the interactions among the CO_2, water and the rock minerals leading to geochemical changes [13]. The changes in the characteristics of the water-saturated porous domain as a result of the contamination by CO_2 are expected to be different depending on whether the contamination takes place in carbonate or silicate aquifer. It is therefore important to understand the behaviours of the CO_2-contaminated water in porous media together with the influence of mineral content of the porous media. The results of the investigations of the scenarios described above using geoelectrical, pH and membrane measurement techniques are presented and discussed below for various conditions

corresponding to different geological depths at which potable water aquifers might be found in the geological domain.

3.1 Change in pH of the water-saturated domain contaminated by CO_2

Migration of leaked CO_2 from storage site might encounter potable water aquifer that lie along its path. As such, the change in the pH of the CO_2-contaminated water in the aquifer can be used to monitor this scenario [10], [21], [25]. In the laboratory experiment, the change of pH with time for water-saturated silica sand contaminated by CO_2 is shown in Figure 3 at conditions corresponding to 200m depth (see, Table 2). The scenario in the figure shows the existence of three stages in the profile of pH with time for CO_2-contaminated water in silica sand. Following the start of the experiment, there was a decline in the pH value with time. After this initial decline, the second stage begins with short rise in pH value. This is then followed by the third stage, which is a period of steady state in the pH value, and it remains till the end of the experiment. In the figure, the immediate fall in the pH value at the start of the experiment can be attributed to the quick dissolution of CO_2 in the water in the porous sample. The decrease in pH continues after the start of the experiment before it rises again and finally levels off at the steady pH value, which lasts until the end of the experiment. However, the final steady state value of the pH is still lower than the original pH value of the uncontaminated water.

The behaviour described above can be interpreted as follows. The region of continued reduction of pH indicates the increase in the amount of dissolved CO_2 leading to the formation of carbonic acid, thereby lowering the pH. Increase in the concentration of carbonic acid results in the lowering of pH [13]. The rise of the pH following the initial decline indicates a reverse reaction leading to the formation of aqueous and possibly gaseous CO_2 and water from the carbonic acid. Following the period of forward and reverse reactions, the system attains equilibrium. This is represented by the steady state value of pH, which remains until the end of the experiment. Furthermore, Figure 3 shows the repeatability of the experiments (run 1 and run 2).

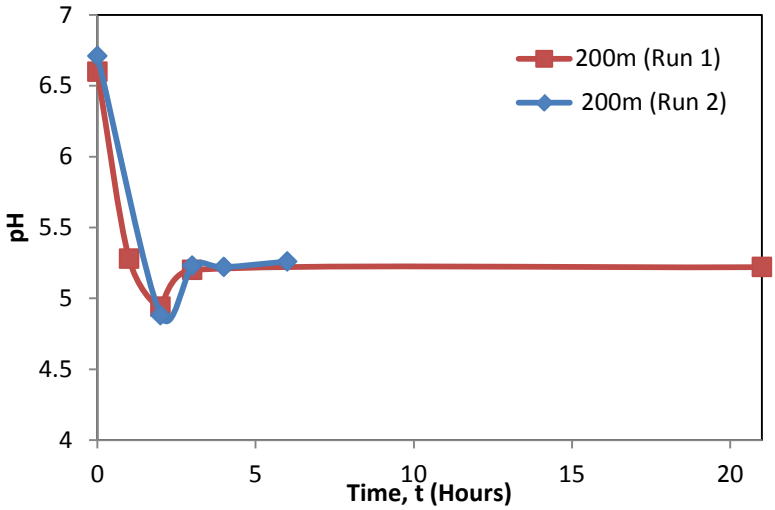

Figure 3: Replicate experimental results showing the three stages of changes in pH for water-saturated silica sand contaminated by CO_2 at conditions corresponding to 200m depth.

Table 3 shows the results of the changes in pH for all the experiments performed in this work under different conditions and in different porous media. The results in the table show the pH values at the start of the experiment and at the steady state. Judging from Figure 3, the pH in the system reaches steady state value quite readily (i.e., at less than 3 hours). The results reported for steady state values in Table 3 were obtained at the end of each of the experiments which often took more than 20 hours. The table shows that the steady state value of pH decreases from the initial value at the start of the experiment, as a result of the CO_2 dissolution in the water-saturated silica sand. The decrease in pH can be seen to be an indication of the formation of carbonic acid as a result of the dissolution of CO_2 in the water. Also, it is shown in the table that the change in pH increases with depth. This implies that the pH change is a function of pressure and temperature because the pressures and temperatures listed in Table 2 are dependent on depth. But, looking at the temperature and pressure values for different depths in Table 2, the temperature only increases by approximately 10% from 50 to 100m depth while the pressure increases by over 100% for the same change in depth. Thus, one can say that the change in pH with depth is mainly due to the effect of pressure. It is known that the dissolution of CO_2 in water increases with pressure [13], [29]–[31].

Table 3: Changes in pH of water-saturated silicate and carbonate porous media in the presence of CO_2 at various depths

Depth (m)	**pH**			
	pH at start		**pH at steady state**	
	Silica	Limestone	Silica	Limestone
50	6.7	7.01	5.34	6.02
100	6.7		5.26	
200	6.7	7.01	5.22	5.85

In the limestone porous domain, the steady state value of pH of the water contaminated by CO_2 also changes with depth. This is also shown in Table 3 for conditions corresponding to the 50 and 200m depths. To understand the influence of mineral contents of the porous medium on the pH of the contaminated water, comparison was made between the behaviours of the CO_2-contaminated water in silica sand and limestone. The properties of the media are already listed in Table 1. As shown in Table 3, the changes in pH value (i.e., percent difference in starting and the steady state pH values) for water-saturated limestone in the presence of CO_2 were approximately 14 and 17% at 50 and 200m depths, respectively. In water-saturated silica sand, the corresponding changes in pH values were 20 and 22%, respectively. Thus, pH change is more severe in silicate than carbonate porous domains. The results indicate that in the presence of CO_2, severe groundwater acidification will occur in non-carbonate aquifers [12].with time still remains higher in limestone than silica sand. This can be attributed to the alkaline nature of the limestone. It is known that alkalinity raises the value of the pH.

3.2 Bulk dielectric constant of the water-saturated domain in the presence of CO_2

Investigations of the CO_2-contaminated water in the porous media using geoelectrical measurement techniques further reveals the responses of the bulk electrical parameters (ε_b and σ_b) with the dissolution of CO_2 in the water-saturated domain. It is known that the bulk electrical parameters of the water-saturated porous media domain change with decrease in the saturation of the wetting phase (water) [16], [27]. But, in the case of CO_2 contamination of the water in porous media, static conditions are envisaged, where there is no noticeable change in the water saturation. Thus, in this work, the behaviours of the geoelectrical

parameters in the contaminated porous media domain are plotted against time instead of the water saturation as in the studies cited above. Figure 4 shows the trend in the bulk dielectric constant (ε_b) for the water-saturated silica sand contaminated by CO_2. There is no sign of change in the ε_b for the entire duration of the experiment. The figure also shows repeatability of the measurements under similar conditions. This is indicated by run 2 in the figure.

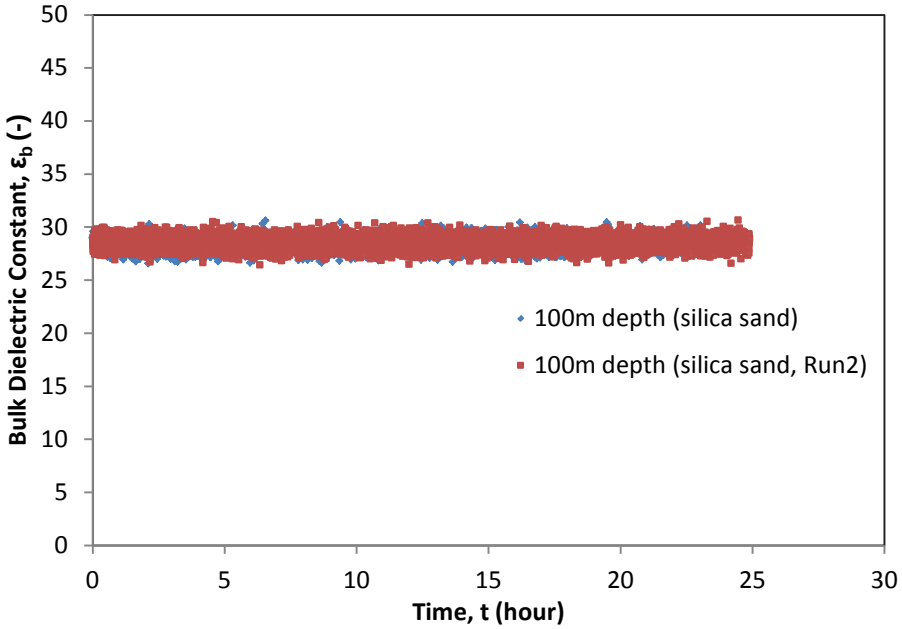

Figure 4: Replicate experiments for bulk dielectric constant of water-saturated silica sand contaminated by CO_2 at conditions corresponding to 100m depth.

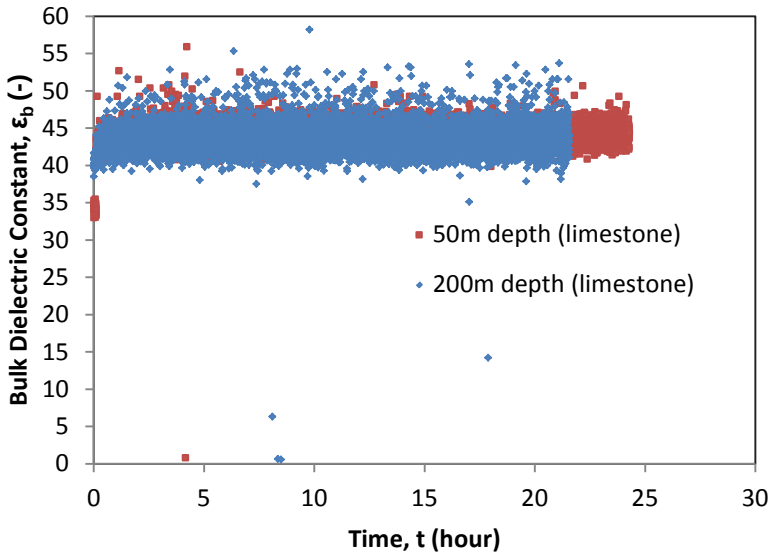

Figure 5: Bulk dielectric constant for water-saturated limestone contaminated by CO_2 at conditions corresponding to 50 and 200m depths.

In addition, Figure 5 shows the ε_b for the water-saturated limestone contaminated by CO_2 at conditions corresponding to 50 and 200m geological depths. The figure shows no sign of change in ε_b at different depths in the limestone.

Thus, one can infer that the ε_b for the water-saturated porous media contaminated by CO_2 does not change with increase in the dissolution of CO_2 in the water. It must be distinguished that investigations in this work was done under static conditions where the saturation of water in porous media domain does not change. This is unlike the work of Plug et al. [27]where the ε_b was shown to vary with change in water saturation as CO_2 displaces the resident water in the porous media. Thus, ε_b is dependent on the flow condition of the two-phase system in the porous medium.

3.3 Bulk electrical conductivity of the water-saturated domain in the presence of CO_2

Another electrical parameter of importance is the electrical conductivity. The behaviour of the bulk electrical conductivity (σ_b) in potable water aquifer contaminated by CO_2 was also examined. Figure 6 shows the replicate experimental results for the σ_b in the water-saturated silica sand contaminated by CO_2. There appears short rise in the σ_b for the system before constant value was attained. This can be interpreted as a period of increase in ionic strength of the pore fluid owing to the dissolution of CO_2, leading to the increase in the electrical conductivity, as a result of the formation of readily-dissociated bicarbonate from the carbonic acid. At the period of increase in σ_b, the reaction seems to produce more bicarbonate from the carbonic acid. The short rise in σ_b can be seen to coincide with the initial period of decrease in the pH shown in Figure 3, where the rate of bicarbonate formation from non-dissociated carbonic acid seems high. This period is characterised with the rise in the ionic concentration of water-saturated porous domain contaminated by CO_2 [13]. Thus, σ_b rises during this period as shown in Figure 6. As the process continues, equilibrium was reached at which the value of σ_b becomes steady as shown in the figure. In the Figure 3, the second stage of short rise in the pH after initial decrease was explained to be due to the reverse formation of aqueous and possibly gaseous CO_2 and water from the carbonic acid. This stage seems to provide ionic equilibrium state in the system, leading to the steady state value in σ_b. Thus, σ_b behaviour in the Figure 6 does not reflect the second stage in pH since ionic species may not change at this period, i.e., second stage of pH change in Figure 3 may be concerned with reverse reaction of non-dissociated carbonic acid, leaving the amount of ionic species from dissociated bicarbonate unchanged. Figure 6 further shows the repeatability of the measurements under similar conditions (indicated by run2).

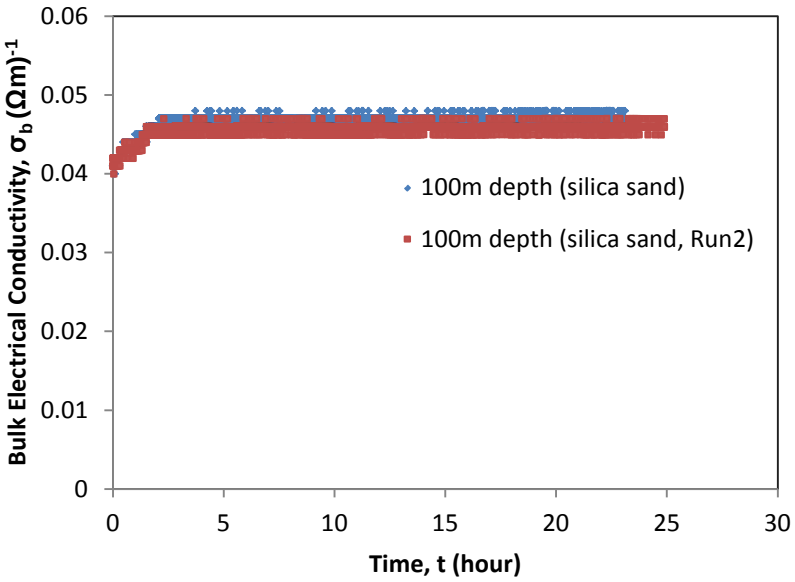

Figure 6: Replicate experiments showing bulk electrical conductivity of water-saturated silica sand contaminated by CO_2 at conditions corresponding to 100m depth.

Similar scenario as above was observed in σ_b for water-saturated limestone contaminated by CO_2. This is shown in Figure 7 for conditions corresponding to 50 and 200m depths (see, Table 2). The σ_b increases with depth. This can be seen as the effect of pressure on σ_b. The results imply that the CO_2 dissolution and the amount of bicarbonate increase with pressure (depth) prior to the attainment of equilibrium. Furthermore, a comparison of Figures 6 and 7 shows that the σ_b in limestone is far higher than in silica sand under similar conditions of injected CO_2. Model by Yang et al. [12] found increasing trend in concentrations of major ions in the carbonate sediment (i.e., limestone). Therefore, mineral dissolution is more pronounced in limestone, leading to higher ion concentration in the domain and, in effect, higher, σ_b.

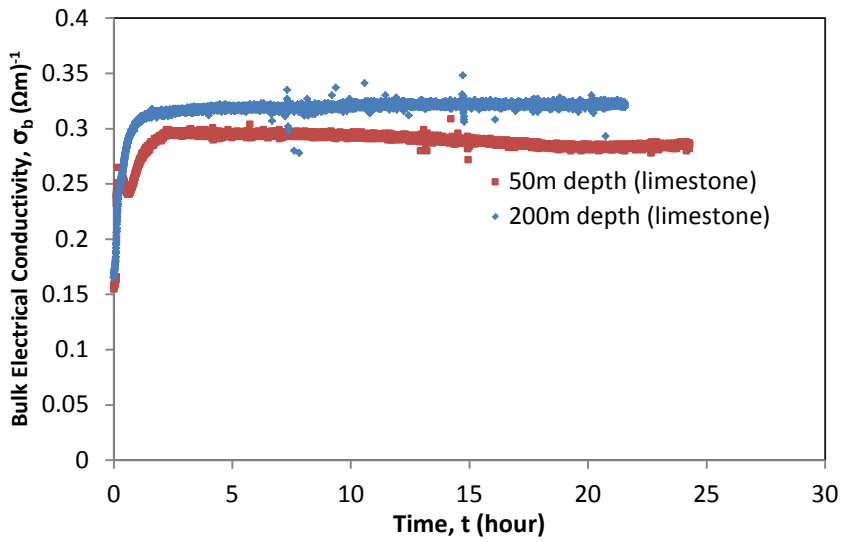

Figure 7: Bulk electrical conductivity of water-saturated limestone at conditions corresponding to 50 and 200m depths.

3.4 Diffusion of CO_2 in the water-saturated domain and its permeation through silicone rubber membrane

When CO_2 contacts the potable water aquifer, contamination of the water will occur via dissolution and diffusion of CO_2 through the water-saturated domain. Keeping this in mind, we would discuss the results of the monitoring of the diffusion process using silicone rubber membrane devised with pressure sensors. The change in the pressure reading on the membrane-sensor system occurring via permeation of the CO_2 through the membrane was recorded as an indicator of the diffusion process.

Figure 8 shows experimental results of CO_2 permeation through silicone rubber membrane at different conditions corresponding to 50, 100, and 200m depths. As the depth increases, the permeation rate increases. The start of the permeation was characterised by rise in the pressure of the permeated gas. At 50m depth, the permeation starts after 8 hours of contamination of the water-saturated domain by CO_2. This reduces to around 4hrs at 100m depth and less than an hour at 200m depth. Thus, the permeation rate of CO_2 through the non-porous membrane increases, as the pressure or depth increases. Therefore, CO_2 leakage and contamination of potable water aquifer can be quickly detected at greater geological depths using the membrane-sensor system, as described above.

The flux of CO_2 through the membrane is shown in Figure 9. The flux values are very small, but the figure shows that the CO_2 flux increases with depth. At 200m depth, the flux values show geometrical rise in comparison to the flux values at 50 and 100m depths. This can be

owing to the ease at which membrane resistance is overcome at greater depth or higher pressure. Therefore, at greater geological depth, flux of CO_2 through non-porous membrane can be easily detected and can give indication of presence of CO_2.

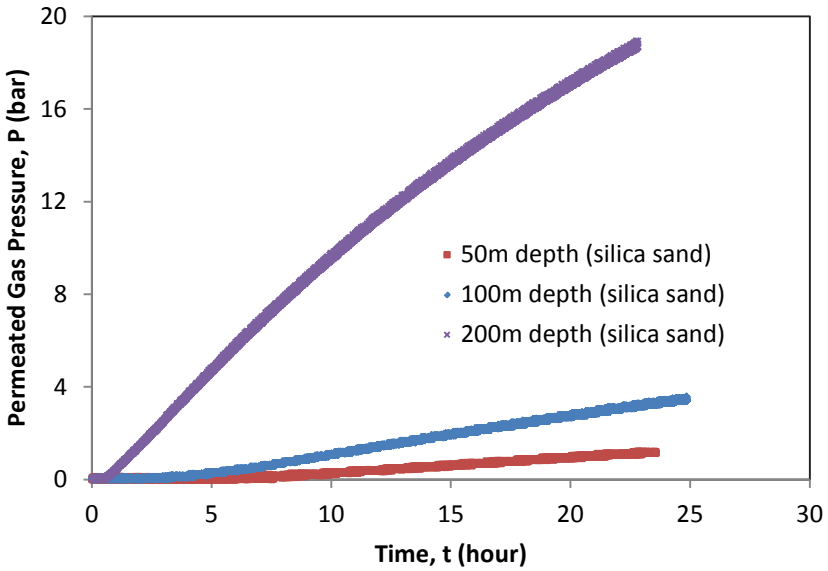

Figure 8: Permeation of CO_2 into silicone rubber membrane via diffusion through water-saturated silica sand.

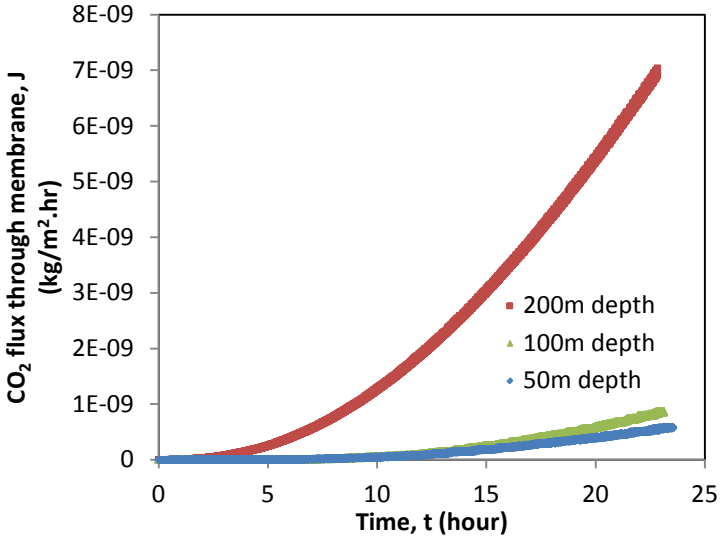

Figure 9: CO_2 flux through the silicone rubber membrane via diffusion through water-saturated silica sand.

3.5 A mathematical expression between pH and σ_b

Above discussions show the existence of a relationship between the pH and σ_b of the porous domain. It was earlier stated that the short rise in σ_b appears to coincide with the initial period of decrease in the pH as shown in Figure 3, which seems to indicate a high rate of

bicarbonate formation from non-dissociated carbonic acid. An assessment of the results shows that the σ_b is dependent on the pH and the initial value of $\sigma_{b.}$ Its dependence on the former is evident in the increase of σ_b as the pH decreases while its dependence on the latter is shown by higher σ_b values in water-saturated limestone than the water-saturated silica sand. Water-saturated limestone domain has higher initial σ_b value. In order to generalise this behaviour one may think of a mathematical expression between these parameters, which is expressed as follows:

$$\sigma_{br} = f(pH_r, \sigma_{bi}) \tag{2}$$

σ_{br} is the ratio of the steady state value of σ_b (i.e., the value of σ_b when the pH is at steady state) to the initial value of σ_b (i.e., σ_{bi}). σ_{bi} is the initial value of σ_b before the injection of CO_2. pH_r is the ratio of the steady state value (i.e., pH value at steady state) to the initial value of the pH (i.e., the pH value before the injection of CO_2). This arrangement enables the determination of the change in σ_b at different conditions and porous media properties provided the data of the initial σ_b and pH_r are available. An attempt to develop a mathematical expression has been made using the combined data from the experiments involving silica sand and limestone porous domains. A regression has been performed using MATLAB (Matrix Laboratory, Mathworks, Cambridge, UK) and the resulting expression is shown in equation (3):

$$\sigma_{br} = 3.87\sigma_{bi}^{0.42} pH_r^{-0.4} \tag{3}$$

The regression has a R^2 value of 0.997. Comparisons of the results from the experiments and predictions by equation (3) are shown in Figure (10). In the figure, we find that the experimental results and the mathematical predictions by equation (3) match well for different porous media samples at different depths. This gives the possibility that the final σ_b of a water-saturated porous domain into which CO_2 is injected can be determined if the changes in pH and the initial values of σ_b are known.

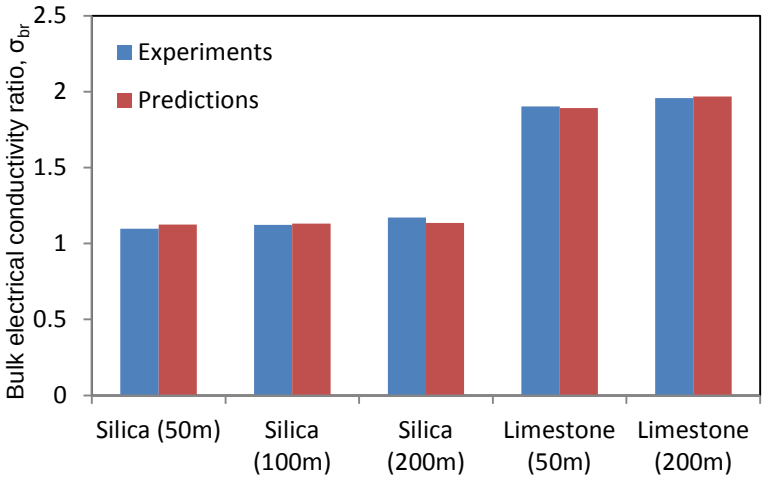

Figure 10: Comparison of the ratios of the bulk electrical conductivity (σ_{br}) from the experiments and mathematical predictions

Above results and discussions examine experimental techniques to monitor plume of CO_2 around the potable water aquifers. Since CO_2 plume resulting from leakage of CO_2 from carbon storage aquifer can migrate through different depths of geological sediments, the studies were conducted at conditions corresponding to different geological depths using geoelectrical, pH and membrane flux parameters. The results showed the applicability of multi-parameter characterization techniques in the monitoring of CO_2-contaminated water in the different aquifers. A mathematical expression developed for the relationship among various parameters can provide estimate of the change in the σ_b and pH of the water-saturated silica sand and the limestone into which CO_2 is injected. However, further studies are needed in the application of the techniques at field scale. Also, there is a need for more experiments to establish a distinguishing criterion between different gases that can permeate the membrane in the subsurface.

4.0 Conclusion

This work looked into the characteristics of potable water contaminated by CO_2 in the silicate and carbonate porous media domain, respectively. The results showed three stages in the profile of pH change with time as CO_2 dissolved and diffused in water-saturated silica sand. The first stage was characterised by rapid decline in the pH from the start of the experiment associated with quick dissolution of CO_2 and the formation of carbonic acid along with bicarbonate. This was followed by the second stage, showing short rise in pH value, which is attributed to the reverse reaction, leading to the formation of aqueous and gaseous CO_2 and water from carbonic acid. The third stage was that of the equilibrium in the forward and the

reverse reactions, marked by steady state in pH value, which remained unchanged till the end of the experiment. The bulk electrical conductivity (σ_b) increased at the contact of the CO_2 with the water-saturated porous media domain in a process attributed to the formation of ionic species, especially bicarbonate from the dissolution of CO_2 in water. The rise in σ_b coincided with the first stage of the change in the pH of the system. The σ_b was higher in limestone than silica sand, and it increased with depth or domain pressure. But, the bulk dielectric constant (ε_b) showed no change with time and pressure. Silicone rubber membrane showed the promise of detecting the diffusion of the CO_2 through the water-saturated domain and the rate of permeation of CO_2 through the membrane was shown to increase with depth. A mathematical relationship developed in this work shows the dependence of σ_b on the pH and initial value of $\sigma_{b.}$

References

[1] D. P. Vuuren, S. Deetman, J. Vliet, M. Berg, B. J. Ruijven, and B. Koelbl, "The role of negative CO2 emissions for reaching 2 °C—insights from integrated assessment modelling," *Clim. Change*, vol. 118, no. 1, pp. 15–27, Feb. 2013.

[2] K. Abidoye, L.K., Das, D.B., Khudaida, "Geological carbon sequestration in the context of two-phase flow in porous media: A review," *Crit. Rev. Environ. Sci. Technol.*, 2014, DOI: 10.1080/10643389.2014.924184 (in press).

[3] K. Khudaida and D. B. Das, "A numerical study of capillary pressure-saturation relationship for supercritical carbon dioxide (CO_2) injection in deep saline aquifer," *Chem. Eng. Res. Des.*, May 2014, DOI: 10.1016/j.cherd.2014.04.020.

[4] Q. Tao and S. L. Bryant, "Well permeability estimation and CO_2 leakage rates," *Int. J. Greenh. Gas Control*, vol. 22, pp. 77–87, Mar. 2014.

[5] P. Humez, P. Audigane, J. Lions, C. Chiaberge, B. W. Division, F. G. Survey, A. C. Guillemin, and O. Cedex, "Modeling of CO_2 leakage up through an abandoned well from deep saline aquifer to shallow fresh groundwaters," vol. 1, pp. 153–181, 2011.

[6] J. M. Nordbotten, M. A. Celia, and S. Bachu, "Analytical solutions for leakage rates through abandoned wells," *Water Resour. Res.*, vol. 40, no. 4, Apr. 2004, doi:10.1029/2003WR002997.

[7] D. Huo and B. Gong, "Discrete Modeling and Simulation on Potential Leakage through Fractures in CO2 Sequestration," in SPE Annual Technical Conference and Exhibition, 19-22 September, 2010, Florence, Italy.

[8] P. Chiquet, D. Broseta, and S. Thibeau, "Wettability alteration of caprock minerals by carbon dioxide," *Geofluids*, vol. 7, no. 2, pp. 112–122, May 2007.

[9] K. Pruess, "Numerical Simulation of CO_2 Leakage from a Geologic Disposal Reservoir , Including Transitions from Super- to Sub-Critical Conditions , and Boiling of Liquid

CO_2." Proceedings, TOUGH Symposium 2003 Lawrence Berkeley National Laboratory, Berkeley, CA, May 12–14 (2003) p. 8

[10] F. Dethlefsen, R. Köber, D. Schäfer, S. A. Al Hagrey, G. Hornbruch, M. Ebert, M. Beyer, J. Großmann, and A. Dahmke, "Monitoring Approaches for Detecting and Evaluating CO2 and Formation Water Leakages into Near-surface Aquifers," *Energy Procedia*, vol. 37, pp. 4886–4893, 2013.

[11] M. Zimmer, J. Erzinger, and C. Kujawa, "The gas membrane sensor (GMS): A new method for gas measurements in deep boreholes applied at the CO2SINK site," *Int. J. Greenh. Gas Control*, vol. 5, no. 4, pp. 995–1001, Jul. 2011.

[12] C. Yang, Z. Dai, K. D. Romanak, S. D. Hovorka, and R. H. Treviño, "Inverse modeling of water-rock-CO2 batch experiments: Potential impacts on groundwater resources at carbon sequestration sites," *Environ. Sci. Technol.*, vol. 48, no. 5, pp. 2798–2806, 2014.

[13] B. Dafflon, Y. Wu, S. S. Hubbard, J. T. Birkholzer, T. M. Daley, J. D. Pugh, J. E. Peterson, and R. C. Trautz, "Monitoring CO_2 intrusion and associated geochemical transformations in a shallow groundwater system using complex electrical methods," *Environ. Sci. Technol.*, vol. 47, no. 1, pp. 314–321, 2012.

[14] V. P. Drnevich, X. Yu, J. Lovell, and J. Tishmack, "Temperature effects on dielectric constant determined by time domain reflectometry," *Proc. TDR2001*, 2001. Innovative Applications of TDR Technology, Infrastructure Technology Institute, Northwestern University, Evanston, IL, September.

[15] Y. Nakatsuka, Z. Xue, H. Garcia, and T. Matsuoka, "Experimental study on CO_2 monitoring and quantification of stored CO_2 in saline formations using resistivity measurements," *Int. J. Greenh. Gas Control*, vol. 4, no. 2, pp. 209–216, 2010.

[16] V. P. Drnevich, X. Yu, J. Lovell, and J. Tishmack, "Temperature effects on dielectric constant determined by time domain reflectometry," *Proc. TDR2001*, 2001. Innovative Applications of TDR Technology, Infrastructure Technology Institute, Northwestern University, Evanston, IL, September.

[17] D. B. Das, B. S. Gill, L. K. Abidoye, and K. J. Khudaida, "A numerical study of dynamic capillary pressure effect for supercritical carbon dioxide-water flow in porous domain," *AIChE J.*, 2014, DOI: 10.1002/aic.14577.

[18] D. N. Espinoza, S. H. Kim, and J. C. Santamarina, "CO_2 Geological Storage − Geotechnical Implications," vol. 15, pp. 707–719, 2011.

[19] R. Shukla, P. Ranjith, A. Haque, and X. Choi, "A review of studies on CO_2 sequestration and caprock integrity," *Fuel*, vol. 89, no. 10, pp. 2651–2664, Oct. 2010.

[20] K. Verwer, G. P. Eberli, and R. J. Weger, "Effect of pore structure on electrical resistivity in carbonates," *Am. Assoc. Pet. Geol. Bull.*, vol. 95, no. 2, pp. 175–190, 2011.

[21] M. G. Little and R. B. Jackson, "Potential impacts of leakage from deep CO_2 geosequestration on overlying freshwater aquifers.," *Environ. Sci. Technol.*, vol. 44, no. 23, pp. 9225–32, Dec. 2010.

[22] J. Bear, *Dynamics of fluids in porous media*. Courier Dover Publications, 2013, ISBN-13:978-0-486-65675-5.

[23] W.-J. Plug and J. Bruining, “Capillary pressure for the sand–CO_2–water system under various pressure conditions. Application to CO2 sequestration,” *Adv. Water Resour.*, vol. 30, no. 11, pp. 2339–2353, Nov. 2007.

[24] M. G. Best, *Igneous and Metamorphic Petrology*. John Wiley & Sons, 2013, ISBN 1-40510-588-7..

[25] H. Lamert, H. Geistlinger, U. Werban, C. Schütze, A. Peter, G. Hornbruch, A. Schulz, M. Pohlert, S. Kalia, M. Beyer, and others, “Feasibility of geoelectrical monitoring and multiphase modeling for process understanding of gaseous CO_2 injection into a shallow aquifer,” *Environ. Earth Sci.*, vol. 67, no. 2, pp. 447–462, 2012.

[26] G. C. TOPP, W. D. ZEBCHUK, J. L. DAVIS, and W. G. BAILEY, “THE MEASUREMENT OF SOIL WATER CONTENT USING A PORTABLE TDR HAND PROBE,” *Can. J. Soil Sci.*, vol. 64, no. 3, pp. 313–321, Aug. 1984.

[27] W. J. Plug, L. M. Moreno, J. Bruining, and E. C. Slob, “Simultaneous Measurement of Capillary Pressure and Dielectric Constant in Porous Media,” *PIERS Online*, vol. 3, no. 4, pp. 549–553, 2007.

[28] S. Salehi Shahrabi, H. R. Mortaheb, J. Barzin, and M. R. Ehsani, “Pervaporative performance of a PDMS/blended PES composite membrane for removal of toluene from water,” *Desalination*, vol. 287, pp. 281–289, Feb. 2012.

[29] A. N. Omambia and Y. Li, “Numeric modeling of carbon dioxide sequestration in deep saline aquifers in Wangchang Oilfield-Jianghan Basin, China,” *J. Am. Sci.*, vol. 6, no. 8, 2010.

[30] Z. Duan and R. Sun, “An improved model calculating CO_2 solubility in pure water and aqueous NaCl solutions from 273 to 533 K and from 0 to 2000 bar,” *Chem. Geol.*, vol. 193, no. 3, pp. 257–271, 2003.

[31] Y.-B. Chang, B. Coats, and J. Nolen, “A Compositional Model for CO_2 Floods Including CO_2 Solubility in Water,” *SPE Reserv. Eval. Eng.*, vol. 1, no. 2, pp. 155–160, Apr. 1998.

Graphical abstract

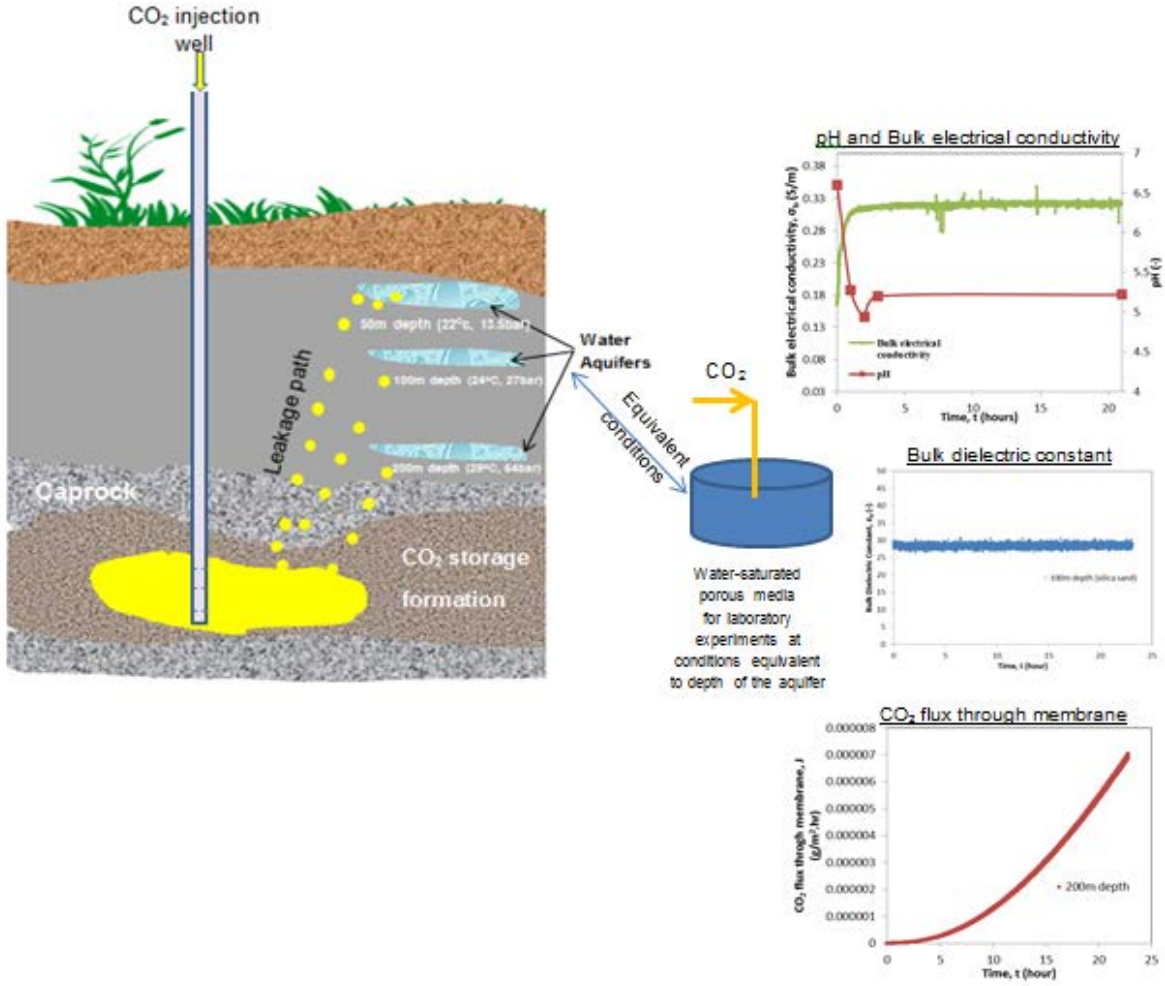

Highlights

- Behaviour of water-saturated porous media contaminated by CO_2 investigated.
- Investigations conducted at conditions equivalent to different aquifer depths.
- Behaviour of pH in the contaminated domain investigated.
- Behaviour of bulk electrical conductivity investigated.
- Behaviour of bulk dielectric constant investigated.
- CO_2 diffusion in the water-saturated domain monitored by flux of CO_2 in membrane
- Investigations conducted for silicate and carbonate porous domains